

Heavy Quarkonium at finite temperature

Nora Brambilla

Physik-Department, Technische Universität München, James-Franck-Str. 1, 85748 Garching, Germany

Abstract. I discuss quarkonium physics at finite temperature in the framework of nonrelativistic effective field theories.

Keywords: Heavy Quarks, Effective Field Theories, QCD at finite temperature, Quark Gluon Plasma

PACS: 12.38.-t, 11.10.Wx, 25.75.Nq

QUARKONIUM AS A PROBE OF QUARK GLUON PLASMA FORMATION

The study of quarkonium in media has recently undergone crucial developments (see e.g. [1]). Large datasets from heavy-ion collisions have recently become available at RHIC displaying new features related to the quark gluon plasma formation characteristics like the particular structure of jet quenching and the very low viscosity to entropy ratio. In particular the quark gluon plasma looks more like a liquid than a plasma and the use of perturbative expansion appears to be justified only at temperature bigger than the deconfinement one.

The suppression of quarkonium production in the hot medium remains one of the cleanest and most relevant probe of deconfined matter. However, the use of quarkonium yields as a hot-medium diagnostic tool has turned out to be quite challenging for several reasons.

Quarkonium production has already been found to be suppressed in proton-nucleus collisions by cold-nuclear-matter effects, which themselves require dedicated experimental and theoretical attention. Recombination effects may play an additional role and thus transport properties may become relevant to be considered. Finally, the heavy quark-antiquark interaction at finite temperature T has to be obtained from QCD [2, 1].

THE HEAVY QUARK INTERACTION AT FINITE T

Since the publication of the famous paper [3] of Matsui and Satz arguing that color screening in a deconfined QCD medium could destroy all $Q\bar{Q}$ bound states at sufficiently high temperatures, there has been considerable interest in studying the interaction between a heavy quark and a heavy antiquark in hot media. The expectation was that the linearly confining potential of zero temperature would get replaced by a Debye-screened potential at high temperatures [3]. However up to very recent times no proper tool to define and calculate the quarko-

onium potential at finite T was developed. Most of the investigations have been performed with phenomenological potentials whose behaviour was inspired by lattice calculations of the free energy. Color screening is indeed studied on the lattice by calculating the spatial correlation functions of a static quark and antiquark in a color-singlet state which propagates in Euclidean time from $\tau = 0$ to $\tau = 1/T$, where T is the temperature (see e.g. [1, 4, 5] for reviews). Lattice calculations of this quantity with dynamical quarks have been also reported. The logarithm of the singlet correlation function is called the singlet free energy. In the zero-temperature limit the singlet free energy coincides with the zero-temperature potential. Moreover at sufficiently short $Q\bar{Q}$ distances, the singlet free energy is temperature independent and equal to the zero-temperature potential, while for large distance it shows a flattening behaviour that is thought to be related to the screening effect. The range of interaction decreases with increasing temperature. For temperatures above the transition temperature, T_c , the heavy-quark interaction range becomes comparable to the charmonium radius. Based on this general observation, one would expect that the charmonium states, as well as the excited bottomonium states, do not remain bound at temperatures just above the deconfinement transition, and this referred to as quarkonium *dissociation* or quarkonium *melting*. The free energy is extracted on the lattice typically from a calculation of the quark-antiquark Polyakov loop correlator. There are singlet and octet channels that are gauge dependent and one can define also an average gauge-independent free energy. The three different channels show a different dependency on the $Q\bar{Q}$ separation and thus lead to different binding energies when used as phenomenological potentials in the Schrödinger equation [5]. There is a huge literature using the singlet free energy or the corresponding internal energy to calculate quarkonium energies at finite T and reconstructing the lattice meson correlation functions to understand which one fits better.

It is therefore very important to find a theoretical framework that can give us the definition of what is the

$Q\bar{Q}$ potential at finite T and a calculation tool. This is realized by constructing an appropriate effective field theory (EFT).

For observables only sensitive to gluons and light quarks, a very successful EFT called Hard Thermal Loop (HTL) effective theory has been derived in the past [6] by integrating out the hardest momenta proportional to T from the dynamics. However, considering also heavy quarkonium in the hot QCD medium, one has to consider in addition to the thermodynamical scales in T also the scales of the nonrelativistic bound state and the situation becomes more complicate.

In the last few years, there has been a remarkable progress in addressing the problem of outlining an EFT framework for quarkonium at finite temperature and in rigorously defining the quarkonium potential. In [11, 12], the static potential was calculated in the regime $T \gg 1/r \gtrsim m_D$, where m_D is the Debye mass and r the quark-antiquark distance, by performing an analytical continuation of the Euclidean Wilson loop to real time. The calculation was done in the weak-coupling resummed perturbation theory. The imaginary part of the gluon self energy gives an imaginary part to the static potential and hence a thermal width to the quark-antiquark bound state. In the same framework, the dilepton production rate for charmonium and bottomonium was calculated in [13, 14]. In [15], static particles in real-time formalism were considered and the potential for distances $1/r \sim m_D$ was derived for a hot QED plasma. The real part of the static potential was found to agree with the singlet free energy and the damping factor with the one found in [11]. In [16], a study of bound states in a hot QED plasma was performed in a non-relativistic EFT framework. In particular, the hydrogen atom was studied for temperatures ranging from $T \ll m\alpha^2$ to $T \sim m$, where the imaginary part of the potential becomes larger than the real part and the hydrogen ceases to exist. The same study has been extended to muonic hydrogen in [17], providing a method to estimate the effects of a finite charm quark mass on the dissociation temperature of bottomonium. In the next sections we report our work in the construction of an EFT description of heavy quarkonium at finite T . We study the real-time evolution of a static quark-antiquark pair in a medium of gluons and light quarks at finite temperature. For temperatures ranging from values larger to smaller than the inverse distance of the quark and antiquark, and at short distances, we derive the potential between the two static sources, and calculate their energy and thermal decay width. We will see in particular that the EFT enables us to give both a proper definition of the heavy quarkonium potential inside a hot medium and solid calculation tools to obtain it (at least in the weak coupling situation).

AN EFT FRAMEWORK

An EFT framework in real time and weak coupling for quarkonium at finite temperature was developed in [18] working in real time and in the regime of small coupling g , so that $gT \ll T$ and $v \sim \alpha_s$, which is expected to be valid for tightly bound states: $\Upsilon(1S)$, J/ψ ,

Quarkonium in a medium is characterized by different energy and momentum scales. There are the scales of the non-relativistic bound state: (v is the relative heavy-quark velocity): m , the heavy quark mass, mv , the scale of the typical inverse distance between the heavy quark and antiquark, mv^2 , the scale of the typical binding energy or potential and lower energy scale. Furthermore there are the thermodynamical scales: the temperature T , the inverse of the screening length of the chromoelectric interactions, i.e. the Debye mass m_D ($\sim gT$ in the perturbative regime) and lower scales, which we will neglect in the following.

If these scales are hierarchically ordered, then we may expand physical observables in the ratio of such scales. If we separate explicitly the contributions from the different scales at the Lagrangian level this amounts to substituting QCD with a hierarchy of EFTs, which are equivalent to QCD order by order in the expansion parameters. At zero temperature the EFTs that follow from QCD by integrating out the scales m and mv are called respectively Non-relativistic QCD (NRQCD) [7] and potential NRQCD (pNRQCD) [8, 10].

We assume that the temperature is high enough that $T \gg gT \sim m_D$ holds but also that it is low enough for $T \ll m$ and $1/r \sim mv \gtrsim m_D$ to be satisfied, because for higher temperature the bound state ceases to exist. Under these conditions some possibilities are in order. If T is the next relevant scale after m , then integrating out T from NRQCD leads to an EFT that we may name NRQCD_{HTL}, because it contains the hard thermal loop (HTL) Lagrangian [6]. Subsequently integrating out the scale mv from NRQCD_{HTL} leads to a thermal version of pNRQCD that we may call pNRQCD_{HTL}. If the next relevant scale after m is mv , then integrating out mv from NRQCD leads to pNRQCD. If the temperature is larger than mv^2 , then the temperature may be integrated out from pNRQCD leading to a new version of pNRQCD_{HTL} [20]. Note that, as long as the temperature is smaller than the scale being integrated out, the matching leading to the EFT may be performed putting the temperature to zero.

The derived potential V describes the real-time evolution of a quarkonium state in a thermal medium. At leading order, the evolution is governed by a Schrödinger equation. In an EFT framework, the potential follows naturally from integrating out all contributions coming from modes with energy and momentum larger than the binding energy. For $T < V$ the potential is simply the Coulomb potential. Thermal corrections affect the en-

ergy and induce a thermal width to the quarkonium state; these may be relevant to describe the in medium modifications of quarkonium at low temperatures. For $T > V$ the potential gets thermal contributions, which are both real and imaginary.

RESULTS OF THE EFT DESCRIPTION

General findings in this picture are:

- The thermal part of the potential has a real and an imaginary part. The imaginary part of the potential smears out the bound state peaks of the quarkonium spectral function, leading to their dissolution prior to the onset of Debye screening in the real part of the potential (see, e.g. the discussion in [19]). So quarkonium dissociation appears to be a consequence of the appearance of a thermal decay width rather than being due to the color screening of the real part of the potential; this follows from the observation that the thermal decay width becomes as large as the binding energy at a temperature at which color screening may not yet have set in.
- Two mechanisms contribute to the thermal decay width: the imaginary part of the gluon self energy induced by the Landau-damping phenomenon (existing also in QED) [11] and the quark-antiquark color singlet to color octet thermal break up (a new effect, specific of QCD) [18]. Parametrically, the first mechanism dominates for temperatures such that the Debye mass m_D is larger than the binding energy, while the latter dominates for temperatures such that m_D is smaller than the binding energy.
- The obtained singlet thermal potential, V , is neither the color-singlet quark-antiquark free energy nor the internal energy. It has an imaginary part and may contain divergences that eventually cancel in physical observables [18].
- Temperature effects can be other than screening, typically they may appear as power law corrections or a logarithmic dependence [18, 16].
- The dissociation temperature goes parametrically as $\pi T_{\text{melting}} \sim mg^{\frac{4}{3}}$ [16, 19].

THE FREE ENERGY IN THE EFT APPROACH

In [21, 23] the Polyakov loop and the correlator of two Polyakov loops at finite temperature has been calculated at next-to-next-to-leading order in the weak coupling regime and at quark-antiquark distances shorter than the inverse of the temperature and for Debye mass larger

than the Coulomb potential. The calculation has been performed also in the EFT framework [21] and a relation between the Polyakov loop correlator and the singlet and octet quark-antiquark correlator [18] has been established in this setup.

CALCULATION OF BOTTOMONIUM PROPERTIES AT LHC

The EFT provides a clear definition of the potential and a coherent and systematical setup to calculate the masses and widths of the lowest quarkonium resonances at finite temperature. In [22] heavy quarkonium energy levels and decay widths in a quark-gluon plasma, below the melting temperature at a temperature T and screening mass m_D satisfying the hierarchy

$$m \gg m\alpha_s \gg \pi T \gg m\alpha_s^2 \gg m_D, \quad (1)$$

have been calculated at order $m\alpha_s^5$. This implies that $mg^3 \gg T \gg mg^4$ and that πT is lower than πT_{melting} , i.e. quarkonium exists in the plasma. We will further assume that all these scales are larger than Λ_{QCD} and that a weak-coupling expansion is possible for all of them. Finally, in order to produce an expression for the spectrum that is accurate up to order $m\alpha_s^5$, we will assume that $[m_D/(m\alpha_s^2)]^4 \ll g$.

This situation may be relevant for bottomonium $1S$ states ($\Upsilon(1S)$, η_b) at the LHC, for which it may hold $m_b \approx 5 \text{ GeV} > m_b\alpha_s \approx 1.5 \text{ GeV} > \pi T \approx 1 \text{ GeV} > m\alpha_s^2 \approx 0.5 \text{ GeV} \gtrsim m_D$.

We work in the real-time formalism, that allows us to develop a treatment of the quarkonium in the thermal bath very similar to the EFT framework developed for zero temperature [10]. We integrate out the mass and the relative momentum arriving at pNRQCD. According to the hierarchy (1), both these scales are larger than T , which, therefore, may be set to zero in the matching to the EFT. As a consequence, the Lagrangians of NRQCD and pNRQCD are the same as at zero temperature.

Integrating out T from pNRQCD modifies pNRQCD into hard-thermal loop (HTL) pNRQCD, pNRQCD_{HTL}, [18, 20]. With respect to pNRQCD, the pNRQCD_{HTL} Lagrangian gets relevant modifications in two parts. First, the Yang–Mills Lagrangian gets an additional HTL part [6]. This, for instance, modifies the longitudinal gluon propagator in Coulomb gauge into ($k^2 \equiv \mathbf{k}^2$)

$$\frac{i}{k^2} \rightarrow \frac{i}{k^2 + m_D^2} \left(1 - \frac{k_0}{2k} \ln \frac{k_0 + k \pm i\eta}{k_0 - k \pm i\eta} \right), \quad (2)$$

where “+” identifies the retarded and “−” the advanced propagator. Second, the potentials get in addition to the Coulomb potential, which is the potential inherited from pNRQCD, a thermal part, that we call δV .

Potential, energy and decay width

In the following, we will provide the thermal corrections to the color-singlet quark-antiquark potential, the thermal corrections to the spectrum and the thermal decay width, aiming at a precision of the order of $m\alpha_s^5$.

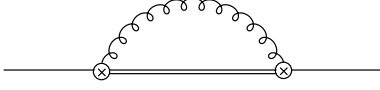


FIGURE 1. The single line stands for a quark-antiquark color-singlet propagator, the double line for a quark-antiquark color-octet propagator and the circle with a cross for a chromo-electric dipole interaction.

Integrating out the scale T

The relevant diagram contributing to the potential is shown in Fig. 1. It reads

$$-ig^2 \frac{4}{3} \frac{r^i}{D-1} \mu^{4-D} \int \frac{d^D k}{(2\pi)^D} \frac{i}{E - h_o - k_0 + i\eta} \times [k_0^2 D_{ii}(k_0, k) + k^2 D_{00}(k_0, k)] r^i, \quad (3)$$

where $D_{\mu\nu}$ stands for the gluon propagator, $h_o = \mathbf{p}^2/m + \alpha_s/(6r)$ is the octet Hamiltonian and the loop integral has been regularized in dimensional regularization ($D = 4 + \varepsilon$ and μ is the subtraction point). In the loop integral, we integrate over the momentum region $k_0 \sim T$ and $k \sim T$. Since $T \gg (E - h_o)$, we may expand

$$\frac{i}{E - h_o - k_0 + i\eta} = \frac{i}{-k_0 + i\eta} - i \frac{E - h_o}{(-k_0 + i\eta)^2} + i \frac{(E - h_o)^2}{(-k_0 + i\eta)^3} - i \frac{(E - h_o)^3}{(-k_0 + i\eta)^4} + \dots \quad (4)$$

The real part of the thermal correction to the color-singlet potential reads

$$\text{Re } \delta V_s(r) = \frac{4\pi}{9} \alpha_s^2 r T^2 + \frac{8\pi}{9m} \alpha_s T^2 + \frac{4\alpha_s I_T}{3\pi} \left[-\frac{9}{8} \frac{\alpha_s^3}{r} - \frac{17}{3} \frac{\alpha_s^2}{mr^2} + \frac{4}{9} \frac{\pi \alpha_s}{m^2} \delta^3(\mathbf{r}) + \frac{\alpha_s}{m^2} \left\{ \nabla_{\mathbf{r}}^2, \frac{1}{r} \right\} \right] - 2\zeta(3) \frac{\alpha_s}{\pi} r^2 T m_D^2 + \frac{8}{3} \zeta(3) \alpha_s^2 r^2 T^3, \quad (5)$$

$$I_T = \frac{2}{\varepsilon} + \ln \frac{T^2}{\mu^2} - \gamma_E + \ln(4\pi) - \frac{5}{3}, \quad (6)$$

$$m_D^2 = g^2 T^2 \left(1 + \frac{n_f}{6} \right), \quad (7)$$

where the first line of Eq. (5) is of order $g^2 r^2 T^3 \times E/T$ and comes from the second term in Eq.(2); the second one is of order $g^2 r^2 T^3 \times (E/T)^3$ and come from the

fourth term in Eq.(4), and the third one, is of order $g^2 r^2 T^3 \times (m_D/T)^2$, comes from a self energy insertion inside the gluon propagator in diagram Fig. 1; n_f is the number of light quarks.

The imaginary part of the color-singlet potential, comes from the imaginary part of the self energy graph mentioned above and reads

$$\text{Im } \delta V_s(r) = \frac{2}{9} \alpha_s r^2 T m_D^2 \left(-\frac{2}{\varepsilon} + \gamma_E + \ln \pi - \ln \frac{T^2}{\mu^2} + \frac{2}{3} - 4 \ln 2 - 2 \frac{\zeta'(2)}{\zeta(2)} \right) + \frac{16\pi}{9} \ln 2 \alpha_s^2 r^2 T^3. \quad (8)$$

This contribution, which may be traced back to the Landau-damping phenomenon, is of order $g^2 r^2 T^3 \times (m_D/T)^2$.

Evaluating $\text{Re } \delta V_s(r)$ and $\text{Im } \delta V_s(r)$ on a quarkonium state with quantum numbers n and l , we obtain the thermal correction to the energy, $\delta E_{n,l}^{(T)}$, and the thermal width, $\Gamma_{n,l}^{(T)}$, coming from the scale T :

$$\delta E_{n,l}^{(T)} = \frac{2\pi}{9} \alpha_s^2 T^2 a_0 [3n^2 - l(l+1)] + \frac{8\pi}{9m} \alpha_s T^2 + \frac{E_n I_T \alpha_s^3}{3\pi} \left\{ -\frac{32}{27} \frac{\delta_{l0}}{n} + \frac{200}{3} \frac{1}{n(2l+1)} - \frac{16}{3} \frac{1}{n^2} + \frac{27}{4} \right\} + \left(-\zeta(3) \frac{\alpha_s}{\pi} T m_D^2 + \frac{4}{3} \zeta(3) \alpha_s^2 T^3 \right) a_0^2 n^2 [5n^2 + 1 - 3l(l+1)], \quad (9)$$

$$\Gamma_{n,l}^{(T)} = \left[-\frac{2}{9} \alpha_s T m_D^2 \left(-\frac{2}{\varepsilon} + \gamma_E + \ln \pi - \ln \frac{T^2}{\mu^2} + \frac{2}{3} - 4 \ln 2 - 2 \frac{\zeta'(2)}{\zeta(2)} \right) - \frac{16\pi}{9} \ln 2 \alpha_s^2 T^3 \right] a_0^2 n^2 [5n^2 + 1 - 3l(l+1)], \quad (10)$$

where $E_n = -\frac{1}{ma_0^2 n^2} = -\frac{4m\alpha_s^2}{9n^2}$ and $a_0 = \frac{3}{2m\alpha_s}$.

Integrating out the scale E

The diagram shown in Fig. 1 also carries contributions coming from the energy scale E . They may be best evaluated in pNRQCD_{HTL} by integrating over the momentum region $k_0 \sim E$ and $k \sim E$ and using HTL gluon propagators. Since $k \sim E \ll T$, we may expand the Bose-Einstein distribution

$$n_B(k) = \frac{T}{k} - \frac{1}{2} + \frac{k}{12T} + \dots; \quad (11)$$

moreover, since $k \sim E \gg m_D$, the HTL propagators can be expanded in $m_D^2/E^2 \ll 1$.

The momentum region $k_0 \sim E$ and $k \sim E$ is characterized by two possible momentum sub-regions. This can be understood by considering the integral

$$\int \frac{d^{D-1}k}{(2\pi)^{D-1}} \int_0^\infty \frac{dk_0}{2\pi} \frac{1}{k_0^2 - k^2 - m_D^2 + i\eta} \left(\frac{1}{E - h_o - k_0 + i\eta} + \frac{1}{E - h_o + k_0 + i\eta} \right). \quad (12)$$

For $k_0 \sim E$ and $k \sim E$, it exhibits an off-shell sub-region, $k_0 - k \sim E$, and a collinear sub-region, $k_0 - k \sim m_D^2/E$. Note that, according to (1), the collinear scale satisfies $mg^4 \gg m_D^2/E \gg mg^6$, i.e. it is smaller than m_D by a factor of $m_D/E \ll 1$ but still larger than the non-perturbative scale g^2T by a factor $T/E \gg 1$.

The thermal correction to the energy, $\delta E_{n,l}^{(E)}$, coming from the scale E , reads

$$\delta E_{n,l}^{(E)} = -\frac{2\pi}{9} \alpha_s T m_D^2 a_0^2 n^2 [5n^2 + 1 - 3l(l+1)]. \quad (13)$$

We note the complete cancellation of the vacuum contribution (which includes the Bethe logarithm) against the thermal contribution originating from the “ $-1/2$ ” term in the expansion of the Bose–Einstein distribution (see Eq. (11)).

The thermal width, $\Gamma_{n,l}^{(E)}$, coming from the scale E , reads


$$\begin{aligned} \Gamma_{n,l}^{(E)} = & 4\alpha_s^3 T - \frac{64}{9m} \alpha_s T E_n + \frac{32}{3} \alpha_s^2 T \frac{1}{mn^2 a_0} \\ & + \frac{2E_n \alpha_s^3}{3} \left\{ -\frac{32}{27} \frac{\delta_{l0}}{n} + \frac{200}{3} \frac{1}{n(2l+1)} - \frac{16}{3} \frac{1}{n^2} + \frac{27}{4} \right\} \\ & - \frac{2}{9} \alpha_s T m_D^2 \left(\frac{2}{\varepsilon} + \ln \frac{E_1^2}{\mu^2} + \gamma_E - \frac{11}{3} - \ln \pi + \ln 4 \right) \\ & a_0^2 n^2 [5n^2 + 1 - 3l(l+1)] + \frac{128 T m_D^2}{81} \frac{\alpha_s^3}{E_n^2} I_{n,l}, \quad (14) \end{aligned}$$

where $I_{1,0} = -0.49673$, $I_{2,0} = 0.64070$, The leading contribution is given by the first three terms, which are of order $\alpha_s^3 T$. This contribution to the thermal width is generated by the possible break up of a quark-antiquark color-singlet state into an unbound quark-antiquark color-octet state: a process that is kinematically allowed only in a medium. The singlet to octet break up is a different phenomenon with respect to the Landau damping. In the situation $E \gg m_D$, the first dominates over the second by a factor $(m\alpha_s^2/m_D)^2$.

Integrating out the scale m_D

The diagram shown in Fig. 1 also carries contributions coming from the energy scale m_D . These contributions are suppressed with respect to the other terms calculated.

TABLE 1. The pattern of IR and UV divergences in the quarkonium spectrum at different energy scales. The final result is finite.

Scale	Vacuum	Thermal
$m\alpha_s$	$\sim m\alpha_s^5 \frac{1}{\varepsilon_{\text{IR}}}$	
T	$\sim m\alpha_s^5 \left(\frac{1}{\varepsilon_{\text{IR}}} - \frac{1}{\varepsilon_{\text{UV}}} \right)$	$\sim -m\alpha_s^5 \frac{1}{\varepsilon_{\text{IR}}}$
$m\alpha_s^2$	$\sim -m\alpha_s^5 \frac{1}{\varepsilon_{\text{UV}}}$	$\sim m\alpha_s^5 \frac{1}{\varepsilon_{\text{UV}}}$

Cancellation of divergences

The thermal corrections to the spectrum and the thermal decay width develop divergences at the different energy scales. These are artifacts of the scale separations and cancel in the final (physical) results.

Concerning the thermal decay width, the divergence at the scale $m\alpha_s^2$ in Eq. (14), which is of ultraviolet (UV) origin, cancels against the infrared (IR) divergence at the scale T in Eq. (10).

In the spectrum, the pattern of divergences is more complicated and is summarized in Tab. 1. The table may be read vertically or horizontally. If read vertically, it shows a typical EFT cancellation mechanism: at the scale $m\alpha_s$ we have non-thermal IR divergences in the potentials, these cancel against non-thermal UV divergences at the scale $m\alpha_s^2$ [24], the non-thermal contribution at the scale T is scaleless and vanishes in dimensional regularization; thermal IR divergences at the scale T cancel against thermal UV divergences at the scale $m\alpha_s^2$. If read horizontally, it shows a cancellation mechanism that is familiar in thermal field theory: at the scale T , thermal IR divergences cancel against non-thermal IR divergences while non-thermal UV divergences cancel against IR divergences that appear in the potentials at the scale $m\alpha_s$; at the scale $m\alpha_s^2$ UV thermal divergences cancel against UV non-thermal divergences. The cancellation between non-thermal and thermal parts is possible because the latter may carry temperature independent terms (see, for instance, the “ $-1/2$ ” term in Eq. (11)). Note that both at the scales T and $m\alpha_s^2$, the spectrum is finite.

Results

For a quarkonium state that satisfies the hierarchy specified in Eq. (1) and in the following discussion, the complete thermal contribution to the spectrum up to $\mathcal{O}(m\alpha_s^5)$ is obtained by summing Eqs. (9) and (13) and

subtracting from the latter the zero-temperature part, this gives

$$\begin{aligned}
\delta E_{n,l}^{(\text{thermal})} &= \frac{2\pi}{9} \alpha_s^2 T^2 a_0 \left[3n^2 - l(l+1) + \frac{8}{3} \right] \\
&+ \frac{E_n \alpha_s^3}{3\pi} \left[\log \left(\frac{2\pi T}{E_1} \right)^2 - 2\gamma_E \right] \\
&\times \left\{ -\frac{32}{27} \frac{\delta_{l0}}{n} + \frac{200}{3} \frac{1}{n(2l+1)} - \frac{16}{3} \frac{1}{n^2} + \frac{27}{4} \right\} \\
&+ \frac{128 E_n \alpha_s^3}{81\pi} L_{n,l} + a_0^2 n^2 [5n^2 + 1 - 3l(l+1)] \\
&\left\{ -\left[\frac{1}{\pi} \zeta(3) + \frac{2\pi}{9} \right] \alpha_s T m_D^2 + \frac{4}{3} \zeta(3) \alpha_s^2 T^3 \right\},
\end{aligned} \tag{15}$$

where $L_{n,l}$ are the QCD Bethe logarithms: $L_{1,0} = -81.5379$, $L_{2,0} = -37.6710$, ... [25].

For a quarkonium state that satisfies the hierarchy specified in Eq. (1) and in the following discussion, the complete thermal width up to $\mathcal{O}(m\alpha_s^5)$ is obtained by summing Eqs. (10) and (14), this gives

$$\begin{aligned}
\Gamma_{n,l}^{(\text{thermal})} &= \left(4 + \frac{832}{81} \frac{1}{n^2} \right) \alpha_s^3 T \\
&+ \frac{2E_n \alpha_s^3}{3} \left\{ -\frac{32}{27} \frac{\delta_{l0}}{n} + \frac{200}{3} \frac{1}{n(2l+1)} - \frac{16}{3} \frac{1}{n^2} + \frac{27}{4} \right\} \\
&- \left[\frac{2}{9} \alpha_s T m_D^2 \left(\ln \frac{E_1^2}{T^2} + 2\gamma_E - 3 - \log 4 - 2 \frac{\zeta'(2)}{\zeta(2)} \right) \right. \\
&+ \frac{16\pi}{9} \ln 2 \alpha_s^2 T^3 \left. \right] a_0^2 n^2 [5n^2 + 1 - 3l(l+1)] \\
&+ \frac{32}{9} \alpha_s T m_D^2 a_0^4 I_{n,l}.
\end{aligned} \tag{16}$$

As a qualitative summary, we observe that, at leading order, the quarkonium masses increase quadratically with T , which implies the same functional increase in the energy of the leptons and photons produced in the electromagnetic decays. Electromagnetic decays occur at short distances $\sim 1/m \ll 1/T$, hence the standard NRQCD factorization formulas hold. At leading order, all the temperature dependence is encoded in the wave function at the origin. The leading temperature correction to it can be read from the potential and is of order $n^4 T^2 / (m^2 \alpha_s)$. Hence, a quadratic dependence on the temperature should be observed in the frequency of produced leptons or photons. Finally, at leading order, a decay width linear with temperature is developed. The mechanism underlying this decay width is the color-singlet to color-octet thermal break-up, which implies a tendency of the quarkonium to decay into a continuum of color-octet states.

ACKNOWLEDGMENTS

We acknowledge financial support from the DFG cluster of excellence ‘‘Origin and structure of the universe’’ (<http://www.universe-cluster.de>).

REFERENCES

1. N. Brambilla *et al.*, arXiv:1010.5827 [hep-ph].
2. N. Brambilla *et al.* [Quarkonium Working Group], arXiv:hep-ph/0412158.
3. T. Matsui and H. Satz, Phys. Lett. B **178** (1986) 416.
4. H. Satz, Rept. Prog. Phys. **63** (2000) 1511; P. Petreczky, Mod. Phys. Lett. A **25** (2010) 3081; A. Mocsy, Nucl. Phys. A **830** (2009) 411C; M. Laine, PoS **LAT2009** (2009) 006,
5. O. Philipsen, Nucl. Phys. A **820** (2009) 33C.
6. E. Braaten and R. D. Pisarski, Nucl. Phys. B **337** (1990) 569; Nucl. Phys. B **339** (1990) 310; Phys. Rev. D **45** (1992) 1827; J. Frenkel and J. C. Taylor, Nucl. Phys. B **334** (1990) 199.
7. W. E. Caswell and G. P. Lepage, Phys. Lett. B **167** (1986) 437; G. T. Bodwin, E. Braaten and G. P. Lepage, Phys. Rev. D **51** (1995) 1125 [Erratum-ibid. D **55** (1997) 5853].
8. A. Pineda and J. Soto, Nucl. Phys. Proc. Suppl. **64** (1998) 428.
9. N. Brambilla, A. Pineda, J. Soto and A. Vairo, Nucl. Phys. B **566** (2000) 275.
10. N. Brambilla, A. Pineda, J. Soto and A. Vairo, Rev. Mod. Phys. **77** (2005) 1423 [arXiv:hep-ph/0410047].
11. M. Laine, O. Philipsen, P. Romatschke and M. Tassler, JHEP **0703** (2007) 054.
12. M. Laine, O. Philipsen and M. Tassler, JHEP **0709** (2007) 066.
13. M. Laine, JHEP **0705** (2007) 028.
14. Y. Burnier, M. Laine and M. Vepsalainen, JHEP **0801** (2008) 043.
15. A. Beraudo, J. P. Blaizot and C. Ratti, Nucl. Phys. A **806**, 312 (2008).
16. M. A. Escobedo and J. Soto, arXiv:0804.0691 [hep-ph].
17. M. A. Escobedo and J. Soto, arXiv:1008.0254 [hep-ph].
18. N. Brambilla, J. Ghiglieri, A. Vairo and P. Petreczky, Phys. Rev. D **78** (2008) 014017.
19. M. Laine, Nucl. Phys. A **820** (2009) 25C.
20. A. Vairo, PoS C **ONFINEMENT8** (2008) 002
21. N. Brambilla, J. Ghiglieri, P. Petreczky and A. Vairo, Phys. Rev. D **82** (2010) 074019
22. N. Brambilla, M. A. Escobedo, J. Ghiglieri, J. Soto and A. Vairo, JHEP **1009** (2010) 038; N. Brambilla, M. A. Escobedo, J. Ghiglieri, and A. Vairo, ‘‘The spin-orbit potential and Poincaré invariance in finite temperature pNRQCD’’, TUM-EFT 15/10 (2010).
23. Y. Burnier, M. Laine and M. Vepsalainen, JHEP **1001** (2010) 054.
24. N. Brambilla, A. Pineda, J. Soto and A. Vairo, Phys. Rev. D **60**, 091502 (1999); B. A. Kniehl and A. A. Penin, Nucl. Phys. B **563**, 200 (1999); N. Brambilla, A. Pineda, J. Soto and A. Vairo, Phys. Lett. B **470**, 215 (1999).
25. B. A. Kniehl, A. A. Penin, V. A. Smirnov and M. Steinhauser, Nucl. Phys. B **635**, 357 (2002).